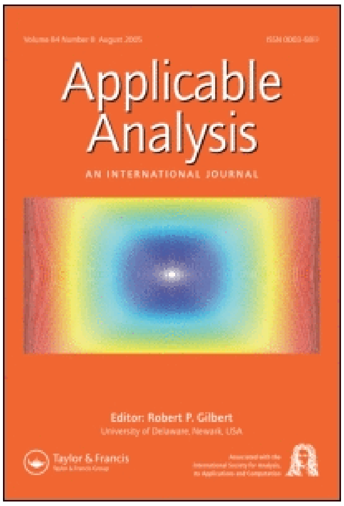

Applicable Analysis
Publication details, including instructions for authors and subscription information:
http://www.informaworld.com/smpp/title~content=t713454076

Studies of a mathematical model for temperature-modulated bioluminescence tomography

Weimin Han [a]; Haiou Shen [b]; Kamran Kazmi [c]; Wenxiang Cong [b]; Ge Wang [b]
[a] Department of Mathematics, University of Iowa, Iowa City, IA 52242, USA [b] Division of Biomedical Imaging, Virginia Tech-Wake Forest University School of Biomedical Engineering and Sciences, Virginia Polytechnic Institute and State University, Blacksburg, VI 24061, USA [c] Department of Mathematics, University of Wisconsin, Oshkosh, WI 54901, USA

Online Publication Date: 01 February 2009

To cite this Article Han, Weimin, Shen, Haiou, Kazmi, Kamran, Cong, Wenxiang and Wang, Ge(2009)'Studies of a mathematical model for temperature-modulated bioluminescence tomography',Applicable Analysis,88:2,193 — 213

To link to this Article: DOI: 10.1080/00036810802713834

URL: http://dx.doi.org/10.1080/00036810802713834

Applicable Analysis
Vol. 88, No. 2, February 2009, 193–213

Taylor & Francis
Taylor & Francis Group

Studies of a mathematical model for temperature-modulated bioluminescence tomography

Weimin Han[a]*, Haiou Shen[b], Kamran Kazmi[c],
Wenxiang Cong[b] and Ge Wang[b]

[a]*Department of Mathematics, University of Iowa, Iowa City, IA 52242, USA;* [b]*Division of Biomedical Imaging, Virginia Tech–Wake Forest University School of Biomedical Engineering and Sciences, Virginia Polytechnic Institute and State University, Blacksburg, VI 24061, USA;* [c]*Department of Mathematics, University of Wisconsin, Oshkosh, WI 54901, USA*

Communicated by Y. Xu

(*Received 12 July 2008; final version received 21 November 2008*)

We introduce and study a mathematical model for temperature-modulated bioluminescence tomography (TBT). The model is capable of self-adjusting values of experimental parameters that are used in the formulation. Major theoretical results of this article include: Solution existence of the model, convergence of numerical solutions, an iterative scheme based on linearization, studies of the solution limiting behaviours when normalized total energy function and/or some or all the energy percentages in individual spectral bands are known exactly. Several numerical examples are included to illustrate the improvement of the accuracy of the reconstructed bioluminescent source distribution due to the employment of measurements from multiple temperature distributions.

Keywords: temperature-modulated bioluminescence tomography (TBT); solution existence; finite element method; convergence; limiting behaviour

1. Introduction

In the past several years, molecular imaging has been rapidly developed to study physiological and pathological processes *in vivo* at the cellular and molecular levels [1,2]. Among molecular imaging modalities, optical imaging has attracted major attention for its unique advantages, especially performance and cost-effectiveness [3–5]. Among various optical molecular imaging techniques, the fluorescence molecular tomography (FMT) [6] and the bioluminescence tomography (BLT) [7–9] are two emerging and complementary modes. In contrast to fluorescent imaging, bioluminescent imaging has unique capabilities in probing molecular and cellular processes. Furthermore, there is no or little background auto-fluorescence with bioluminescent imaging. With BLT, quantitative and localized analyses on a bioluminescent source distribution become feasible in a mouse, which reveal

*Corresponding author. Email: whan@math.uiowa.edu

ISSN 0003–6811 print/ISSN 1563–504X online

DOI: 10.1080/00036810802713834
http://www.informaworld.com

information important for numerous biomedical studies. Some uniqueness results for the BLT problem are given in [8]. A comprehensive theoretical and numerical analysis of the BLT problem is performed in [10]. More theoretical investigations and numerical solutions of the BLT problem are reported in [11–14]. A further step along the direction of BLT development is multi-spectral bioluminescence tomography (MBT) that uses multi-spectral measurement data in reconstructing the bioluminescent source distribution. Some theoretical studies of MBT, including results from numerical simulations, can be found in [15] for a particular formulation. A general framework for MBT is introduced and analysed in [16]. See [17] for a summary account.

Inspired by the experimental results reported in [18] that bioluminescent spectra can be significantly affected by temperature, the temperature-modulated bioluminescence tomography (TBT) was proposed in [19] for more accurate reconstruction of the bioluminescent source distribution. The purpose of the current article is to establish a general mathematical framework for the study of TBT and to provide a thorough theoretical investigation. The rest of this article is organized as follows. We describe the TBT problem in Section 2. In Section 3, we introduce the mathematical framework for the study of the TBT problem through minimizing the mismatch between predicted boundary values by boundary value problems and boundary measurements, coupled with regularization on the source distribution function and penalization for the inaccuracy in the normalized total energy function and energy percentage functions. Solution existence issue is addressed in Section 4. Note that the TBT problem can be solved only approximately; so in Section 5, we consider discretization of the TBT problem using the finite element method. The main result there is on convergence of the numerical solutions. Then in Section 7, we explore the limiting behaviour of the solution of our framework as some of the penalization parameters tend to infinity. We report some numerical results on simulation of the TBT problem in Section 8. The numerical results illustrate that using measurements from multiple temperature distributions lead to accuracy improvement in the reconstructed bioluminescent source distribution.

2. Problem description

We denote by $\Omega \subset \mathbb{R}^d$ the domain occupied by a biological medium and by $\Gamma = \partial\Omega$ for its boundary. The integer d refers to the space dimension. In applications, $d = 3$. However, the mathematical theory can be developed for any dimension.

The diffusion boundary value problem at the normal body temperature is

$$-\text{div}(D\nabla u) + \mu u = p\chi_{\Omega_0} \quad \text{in } \Omega, \tag{2.1}$$

$$u + 2AD\partial_\nu u = 0 \quad \text{on } \Gamma = \partial\Omega. \tag{2.2}$$

Here, $D(\boldsymbol{x}) = 1/[3\,(\mu(\boldsymbol{x}) + \mu'(\boldsymbol{x}))]$, $\mu(\boldsymbol{x})$ and $\mu'(\boldsymbol{x})$ are the absorption coefficient and the reduced scattering coefficient, $\partial/\partial\nu$ stands for the outward normal derivative,

$$A(\boldsymbol{x}) = \frac{1 + R(\boldsymbol{x})}{1 - R(\boldsymbol{x})}, \quad R(\boldsymbol{x}) \approx -1.4399\gamma^{-2} + 0.7099\gamma^{-1} + 0.6681 + 0.0636\gamma$$

with γ being the refractive index of the medium, Ω_0 is a subset of Ω, known as the permissible region and χ_{Ω_0} is the characteristic function of Ω_0. The four coefficients $1.4399, \ldots, 0.0636$ are dimensionless and are emperically determined. The homogeneous boundary condition (2.2) corresponds to a dark environment for the experiments.

The purpose is to reconstruct the source function p from multispectral measurements of outgoing photon densities on portions of the boundary Γ, resulted from several sets of experiments with modulated temperatures. Our discussion in this article will be given in the more general context of the multispectral bioluminescence tomography (MBT). In MBT, the optical imaging study is performed with multiple reporters of different spectra for multiple molecular and cellular targets. Multispectral data are measured in spectral bands on the surface of the biological body, which are then employed for the reconstruction of the distributions of multiple biomarkers. For a detailed theoretical analysis of MBT, see [16].

We now introduce the additional symbols necessary for a description of the problem.

In multispectral bioluminescence tomography, the spectrum is divided into certain number of bands, say i_0 bands $\Lambda_1, \ldots, \Lambda_{i_0}$, with

$$\Lambda_i = [\lambda_{i-1}, \lambda_i),\ 1 \le i \le i_0 - 1, \quad \Lambda_{i_0} = [\lambda_{i_0-1}, \lambda_{i_0}].$$

Here, $\lambda_0 < \lambda_1 < \cdots < \lambda_{i_0}$ is a partition of the whole spectrum range. The case of TBT based on the ordinary single spectrum BLT is recovered by setting $i_0 = 1$.

Several experiments are to be performed at different temperature distributions. Denote by j_0 the number of experiments, and for j-th $(1 \le j \le j_0)$ experiment, let $T_j = T_j(\boldsymbol{x})$ be the corresponding temperature distribution in the medium. Experimental results indicate that the photon density satisfies a diffusion differential equation of the form (2.1) with the right-hand side modified by a temperature dependent scaling parameter. Specifically, in the j-th experiment, the portion of the photon density in the spectral band Λ_i is described by the following boundary value problem, adapted from (2.1) and (2.2):

$$-\mathrm{div}(D\nabla u_{ij}) + \mu u_{ij} = \omega(T_j) w_i(T_j) p \chi_{\Omega_0} \quad \text{in } \Omega, \tag{2.3}$$

$$u_{ij} + 2AD\partial_\nu u_{ij} = 0 \quad \text{on } \Gamma. \tag{2.4}$$

Here, ω is the normalized total energy function, w_i is the energy percentage function for the spectral band Λ_i, $1 \le i \le i_0$. The value of ω at the normal body temperature 37°C is set to be 1: $\omega(37) = 1$. At any temperature T, we have

$$\sum_{i=1}^{i_0} w_i(T) = 1.$$

The corresponding multispectral boundary measurements are

$$Q_{ij} = -D\partial_\nu u_{ij} = \frac{1}{2A} u_{ij} \quad \text{on } \Gamma_i. \tag{2.5}$$

Here Γ_i, $1 \le i \le i_0$, are subsets of Γ, where we measure the multispectral outgoing photon densities. These subsets can be the same, and they can be equal to the entire boundary Γ.

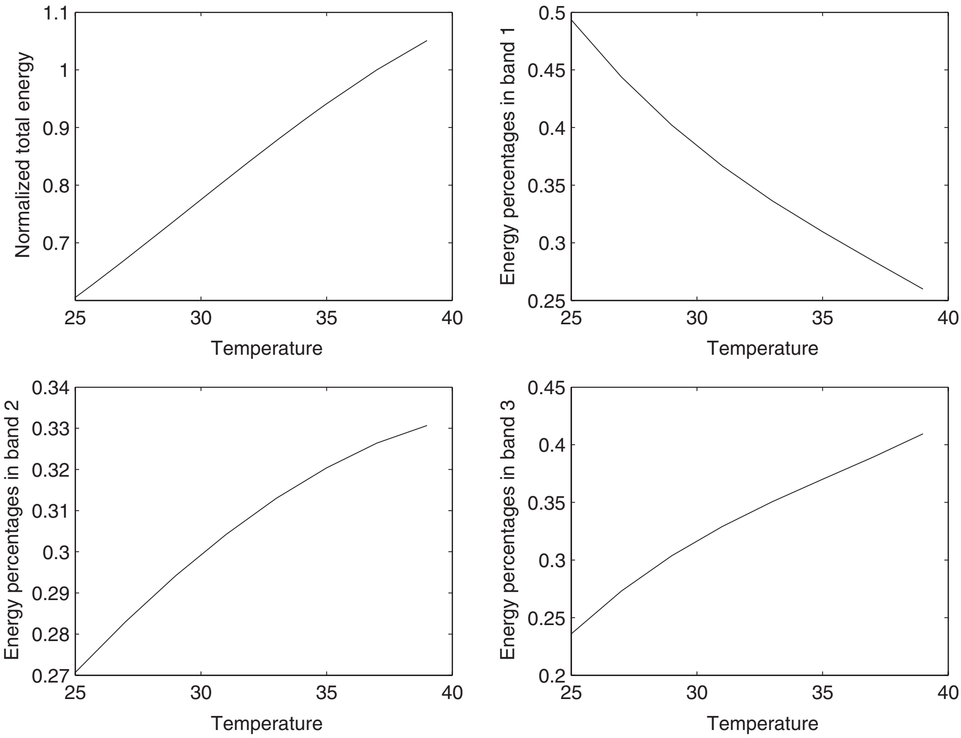

Figure 1. Approximate normalized total energy function and energy percentages in three spectral bands.

Based on prior experimental results, we suppose we know approximate values of ω and $\mathbf{w}=(w_1,\ldots,w_{i_0})^T$; the known approximate values are denoted as $\omega^{(0)}$ and $\mathbf{w}^{(0)}=(w_1^{(0)},\ldots,w_{i_0}^{(0)})^T$ [18,19]. Figure 1 shows graphs of the functions $\omega^{(0)}$ and $w_i^{(0)}$, $1\le i\le 3$, for the temperature range $[25°\mathrm{C}, 39°\mathrm{C}]$. The three spectral bands are $\Lambda_1=[500, 590)$ nm, $\Lambda_2=[590, 625)$ nm, $\Lambda_3=[625, 750]$ nm.

Then the TBT problem is to determine p, ω and $\mathbf{w}$ from (2.3) to (2.5) for $1\le i\le i_0$, $1\le j\le j_0$. As is well-known, this pointwise formulation is ill-posed, see, e.g. [10]. So we study the TBT problem through minimizing the mismatch between predicted boundary values by boundary value problems and boundary measurements, coupled with regularization on the source distribution function and penalization for the inaccuracy in the normalized total energy function and energy percentage functions.

3. A general framework for studying TBT problem

We first make assumptions on the data. Assume $\Omega\subset\mathbb{R}^d$ is a Lipschitz domain, $A(\mathbf{x})\in[A_l, A_u]$ for some constants A_l, $A_u\in(0,\infty)$, $D\in L^\infty(\Omega)$ with $D(\mathbf{x})\ge D_0$ for some constant $D_0>0$, and $\mu\in L^\infty(\Omega)$ with $\mu(\mathbf{x})\ge 0$. Let $f_{ij}=2AQ_{ij}$ and assume $f_{ij}\in L^2(\Gamma_i)$ for $1\le j\le j_0$, $1\le i\le i_0$. Let T_l and T_u be the lower and upper bounds of temperature distributions involved in the experiments. Denote $I_T=(T_l, T_u)$.

We will use the following function spaces: $V=H^1(\Omega)$, $Q_0=L^2(\Omega_0)$, $Q_\Gamma=L^2(\Gamma)$, $Q_{\Gamma_i}=L^2(\Gamma_i)$ for $1\le i\le i_0$, and $V_T=H^1(I_T)$.

In our formulation, unknowns are the source function p, the normalized total energy function ω and the multispectral energy percentage vector function $\boldsymbol{w}=(w_1,\ldots,w_{i_0})^T$. We search for p in a set $Q_p\subset Q_0$, the function ω in the set

$$Q_\omega=\{\omega\in V_T\mid 0\le\omega\le 2\},$$

and $\boldsymbol{w}$ in the set

$$\boldsymbol{Q}_w=\left\{\boldsymbol{w}\in(V_T)^{i_0}\mid 0\le w_i\le 1, 1\le i\le i_0, \sum_i w_i=1\right\}.$$

We assume Q_p is a non-empty, closed, convex set in Q_0. Define the admissible set

$$\boldsymbol{Q}_{ad}=Q_p\times Q_\omega\times\boldsymbol{Q}_w.$$

Then $\boldsymbol{Q}_{ad}$ is a non-empty, closed, convex set in the space $Q_0\times V_T\times(V_T)^{i_0}$.

For any $(p,\omega,\boldsymbol{w})\in Q_0\times V_T\times(V_T)^{i_0}$, we define $u_{ij}=u_j(p,\omega,w_i)\in V$ by

$$\int_\Omega\left(D\nabla u_{ij}\cdot\nabla v+\mu u_{ij}v\right)\mathrm{d}x+\int_\Gamma\frac{1}{2A}u_{ij}v\,\mathrm{d}s=\int_{\Omega_0}\omega(T_j)w_i(T_j)pv\,\mathrm{d}x\quad\forall v\in V \tag{3.1}$$

for $1\le i\le i_0$, $1\le j\le j_0$. Note that (3.1) is a weak form of the boundary value problem (2.3) and (2.4). By the assumptions made on the data D, μ and A, it follows from an application of the Lax–Milgram lemma [20,21] that the solution u_{ij} is uniquely defined by (3.1). For positive numbers ε, M_ω and M_w, we introduce the objective functional

$$\begin{aligned}J(p,\omega,\boldsymbol{w})=&\frac{1}{2}\sum_{i,j}\|u_j(p,\omega,w_i)-f_{ij}\|^2_{Q_{\Gamma_i}}+\frac{\varepsilon}{2}\|p\|^2_{Q_0}\\&+\frac{M_\omega}{2}\|\omega-\omega^{(0)}\|^2_{V_T}+\frac{M_w}{2}\sum_i\|w_i-w_i^{(0)}\|^2_{V_T}.\end{aligned}\tag{3.2}$$

Here ε is meant to be small, whereas M_ω and M_w are meant to be large. Throughout this article, the indices i and j range between 1 and i_0, and 1 and j_0, respectively. We then introduce the following for the study of the reconstruction problem described in Section 2.

Problem 3.1 *Find* $(p,\omega,\boldsymbol{w})\in\boldsymbol{Q}_{ad}$ *such that the objective functional* $J(p,\omega,\boldsymbol{w})$ *is minimal over* $\boldsymbol{Q}_{ad}$.

4. Solution existence

We first present and prove a solution existence result.

Theorem 4.1 *Under the assumptions stated in the beginning of Section* 3 *on the data, Problem* 3.1 *has a solution.*

Proof By definition of the infimum, we have a sequence $\{(p_n,\omega_n,\boldsymbol{w}_n)\}_n\subset\boldsymbol{Q}_{\rm ad}$, $\boldsymbol{w}_n=(w_{1,n},\ldots,w_{i_0,n})^T$, such that

$$J(p_n,\omega_n,\boldsymbol{w}_n)\to\inf_{(p,\omega,\boldsymbol{w})\in\boldsymbol{Q}_{ad}}J(p,\omega,\boldsymbol{w})\quad\text{as }n\to\infty.$$

We note that $\|p_n\|_{Q_0}$, $\|\omega_n\|_{V_T}$ and $\|w_{i,n}\|_{V_T}$, $1 \le i \le i_0$, are all uniformly bounded, independent of n. Denote $u_{ij,n} = u_j(p_n, \omega_n, w_{i,n})$. From the definition (3.1), we deduce that $\|u_{ij,n}\|_V$ is also uniformly bounded, independent of n. Thus, there is a subsequence $\{n'\}$ of the sequence $\{n\}$, and functions $(p_\infty, \omega_\infty, \boldsymbol{w}_\infty) \in \boldsymbol{Q}_{ad}$, $\boldsymbol{w}_\infty = (w_{1,\infty}, \ldots, w_{i_0,\infty})^T$, and $u_{\mathrm{ij},\infty} \in V$ such that as $n' \to \infty$,

$$p_{n'} \rightharpoonup p_\infty \text{ in } Q_0, \tag{4.1}$$

$$\omega_{n'} \rightharpoonup \omega_\infty \text{ in } V_T, \quad \omega_{n'} \to \omega_\infty \text{ in } C(\overline{I_T}), \tag{4.2}$$

$$w_{i,n'} \rightharpoonup w_{i,\infty} \text{ in } V_T, \quad w_{i,n'} \to w_{i,\infty} \text{ in } C(\overline{I_T}),\ 1 \le i \le i_0, \tag{4.3}$$

$$u_{ij,n'} \rightharpoonup u_{ij,\infty} \text{ in } V, \quad u_{ij,n'} \to u_{ij,\infty} \text{ in } Q_\Gamma,\ 1 \le i \le i_0,\ 1 \le j \le j_0. \tag{4.4}$$

Let us show that $u_{\mathrm{ij},\infty} = u_j(p_\infty, \omega_\infty, w_{i,\infty})$. For any $v \in V$, consider the difference

$$\int_{\Omega_0} \omega_{n'}(T_j) w_{i,n'}(T_j) p_{n'} v \,\mathrm{d}x - \int_{\Omega_0} \omega_\infty(T_j) w_{i,\infty}(T_j) p_\infty v \,\mathrm{d}x.$$

It can be rewritten as

$$\int_{\Omega_0} \left[\omega_{n'}(T_j) w_{i,n'}(T_j) - \omega_\infty(T_j) w_{i,\infty}(T_j)\right] p_{n'} v \,\mathrm{d}x + \int_{\Omega_0} \omega_\infty(T_j) w_{i,\infty}(T_j)(p_{n'} - p_\infty) v \,\mathrm{d}x.$$

As $n' \to \infty$, the first term tends to zero because of (4.2) and (4.3), and the second term tends to zero because of (4.1). Therefore,

$$\lim_{n' \to \infty} \int_{\Omega_0} \omega_{n'}(T_j) w_{i,n'}(T_j) p_{n'} v \,\mathrm{d}x = \int_{\Omega_0} \omega_\infty(T_j) w_{i,\infty}(T_j) p_\infty v \,\mathrm{d}x.$$

In the defining relation

$$\int_\Omega \left(D \nabla u_{ij,n'} \cdot \nabla v + \mu u_{ij,n'} v\right) \mathrm{d}x + \int_\Gamma \frac{1}{2A} u_{ij,n'} v \,\mathrm{d}s = \int_{\Omega_0} \omega_{n'}(T_j) w_{i,n'}(T_j) p_{n'} v \,\mathrm{d}x \quad \forall v \in V,$$

let $n' \to \infty$, use the convergence of the right side and the property (4.4) to obtain

$$\int_\Omega \left(D \nabla u_{ij,\infty} \cdot \nabla v + \mu u_{ij,\infty} v\right) \mathrm{d}x + \int_\Gamma \frac{1}{2A} u_{ij,\infty} v \,\mathrm{d}s = \int_{\Omega_0} \omega_\infty(T_j) w_{i,\infty}(T_j) p_\infty v \,\mathrm{d}x \quad \forall v \in V.$$

In other words, $u_{ij,\infty} = u_j(p_\infty, \omega_\infty, w_{i,\infty})$. Using this relation and the properties (4.1)–(4.4), we obtain

$$J(p_\infty, \omega_\infty, \boldsymbol{w}_\infty) \le \liminf_{n' \to \infty} J(p_{n'}, \omega_{n'}, \boldsymbol{w}_{n'}).$$

Therefore,

$$J(p_\infty, \omega_\infty, \boldsymbol{w}_\infty) = \inf_{(p, \omega, \boldsymbol{w}) \in \boldsymbol{Q}_{ad}} J(p, \omega, \boldsymbol{w}),$$

and $(p_\infty, \omega_\infty, \boldsymbol{w}_\infty)$ is a solution of Problem 3.1. ■

Next we present a necessary condition for a solution of Problem 3.1. Associated with an element $(p, \omega, \boldsymbol{w}) \in \boldsymbol{Q}_{ad}$, we introduce the set

$$\boldsymbol{Q}_{ad}(p, \omega, \boldsymbol{w}) = \left\{(\Delta_p, \Delta_\omega, \boldsymbol{\Delta}_w) \in Q_0 \times V_T \times (V_T)^{i_0} \mid (p + \Delta_p, \omega + \Delta_\omega, \boldsymbol{w} + \boldsymbol{\Delta}_w) \in \boldsymbol{Q}_{ad}\right\}.$$

Observe that $\boldsymbol{Q}_{ad}(p,\omega,\boldsymbol{w})$ is a non-empty, closed, convex set in the space $Q_0 \times V_T \times (V_T)^{i_0}$. For any $(p,\omega,\boldsymbol{w}) \in \boldsymbol{Q}_{ad}$, any $(\Delta_p, \Delta_\omega, \boldsymbol{\Delta}_w) \in \boldsymbol{Q}_{ad}(p,\omega,\boldsymbol{w})$ with $\boldsymbol{\Delta}_w = (\Delta_{w_1}, \ldots, \Delta_{w_{i0}})^T$, and $1 \le i \le i_0$, $1 \le j \le j_0$, we define $e_{ij} \equiv e_j(p,\omega,w_i;\ \Delta_p, \Delta_\omega, \Delta_{w_i}) \in V$ by the relation

$$\int_\Omega \big(D\,\nabla e_{ij}\cdot\nabla v + \mu e_{ij} v\big)\mathrm{d}x + \int_\Gamma \frac{1}{2A} e_{ij} v\,\mathrm{d}s$$
$$= \int_{\Omega_0} \big[\omega(T_j)\,\Delta_{w_i}(T_j)\,\Delta_p + w_i(T_j)\,\Delta_\omega(T_j)\,\Delta_p + p\Delta_\omega(T_j)\,\Delta_{w_i}(T_j)\big] v\,\mathrm{d}x \quad \forall v \in V. \tag{4.5}$$

We can show that if $(p,\omega,\boldsymbol{w}) \in \boldsymbol{Q}_{ad}$ is a solution of Problem 3.1, then

$$\sum_{i,j}\big(u_j(p,\omega,w_i) - f_{ij}, e_{ij}\big)_{Q_{\Gamma_i}} + \varepsilon\,(p,\Delta_p)_{Q_0} + M_\omega(\omega - \omega^{(0)}, \Delta_\omega)_{V_T}$$
$$+ M_w \sum_i (w_i - w_i^{(0)}, \Delta_{w_i})_{V_T} \ge 0 \quad \forall(\Delta_p, \Delta_\omega, \boldsymbol{\Delta}_w) \in \boldsymbol{Q}_{ad}(p,\omega,\boldsymbol{w}). \tag{4.6}$$

This relation can be proved similar to that of (2.15) in [11].

5. Numerical approximation

Let $\{\mathcal{T}_{h_\Omega}\}_{h_\Omega}$ be a regular family of finite element partitions of $\overline{\Omega}$, $\{\mathcal{T}_{h_{\Omega 0}}\}_{h_{\Omega 0}}$ a regular family of finite element partitions of $\overline{\Omega_0}$, and $\{\mathcal{T}_{h_T}\}_{h_T}$ a regular family of finite element partitions of $\overline{I_T}$. In the following, we will use the symbol h for the triplet $(h_\Omega, h_{\Omega_0}, h_T)$. By $h \to 0$, we mean $\max\{h_\Omega, h_{\Omega_0}, h_T\} \to 0$.

Corresponding to the partitions $\mathcal{T}_{h_\Omega}$, $\mathcal{T}_{h_{\Omega 0}}$ and $\mathcal{T}_{h_T}$, we construct the related linear finite element space V^{h_Ω}, piecewise constant function space $Q_0^{h_{\Omega 0}}$ and linear finite element space $V_T^{h_T}$. Define $Q_p^{h_{\Omega 0}} = Q_p \cap Q_0^{h_{\Omega 0}}$, $Q_\omega^{h_T} = Q_\omega \cap V_T^{h_T}$, $\boldsymbol{Q}_w^{h_T} = \boldsymbol{Q}_w \cap (V_T^{h_T})^{i_0}$ and the discrete admissible set

$$\boldsymbol{Q}_{ad}^h = Q_p^{h_{\Omega 0}} \times Q_\omega^{h_T} \times \boldsymbol{Q}_w^{h_T}.$$

We assume $\boldsymbol{Q}_{ad}^h$ is non-empty. Then $\boldsymbol{Q}_{ad}^h$ is a closed and convex subset of $\boldsymbol{Q}_{ad}$.

For any $(p^h, \omega^h, \boldsymbol{w}^h) \in \boldsymbol{Q}_{ad}^h$, we define $u_{ij}^h = u_j^h(p^h, \omega^h, w_i^h) \in V^{h_\Omega}$ by

$$\int_\Omega \Big(D\nabla u_{ij}^h \cdot \nabla v^h + \mu u_{ij}^h v^h\Big)\mathrm{d}x + \int_\Gamma \frac{1}{2A} u_{ij}^h v^h \mathrm{d}s = \int_{\Omega_0} \omega^h(T_j)\, w_i^h(T_j)\, p^h v^h\,\mathrm{d}x \quad \forall v^h \in V^{h_\Omega} \tag{5.1}$$

for $1 \le i \le i_0$, $1 \le j \le j_0$. Applying the Lax–Milgram lemma, we deduce that $u_{ij}^h \in V^{h_\Omega}$ is uniquely defined by (5.1). We then introduce a discrete analogue of the functional (3.2):

$$\begin{aligned} J^h(p^h, \omega^h, \boldsymbol{w}^h) &= \frac{1}{2}\sum_{i,j} \|u_j^h(p^h, \omega^h, w_i^h) - f_{ij}\|^2_{Q_{\Gamma_i}} + \frac{\varepsilon}{2}\|p^h\|^2_{Q_0} \\ &\quad + \frac{M_\omega}{2}\|\omega^h - \omega^{(0)}\|^2_{V_T} + \frac{M_w}{2}\sum_i \|w_i^h - w_i^{(0)}\|^2_{V_T}, \end{aligned} \tag{5.2}$$

and that of Problem 3.1:

PROBLEM 5.1 *Find* $(p^h, \omega^h, \boldsymbol{w}^h) \in \boldsymbol{Q}_{ad}^h$ *such that the functional* $J^h(p^h, \omega^h, \boldsymbol{w}^h)$ *is minimal over* $\boldsymbol{Q}_{ad}^h$.

Similar to Problem 3.1, we can show that Problem 5.1 has a solution. Our emphasis here is a convergence result.

THEOREM 5.2 *Let* $\{(p_\infty^h, \omega_\infty^h, \boldsymbol{w}_\infty^h)\}_h$ *be a sequence of discrete solutions,* $h \to 0$. *Then there exist a subsequence* $\{h' = (h'_\Omega, h'_{\Omega_0}, h'_T)\}$ *of* $\{h\}$ *and an element* $(p_\infty^0, \omega_\infty^0, \boldsymbol{w}_\infty^0) \in \boldsymbol{Q}_{ad}^h$ *such that as* $h' \to 0$,

$$p_\infty^{h'} \to p_\infty^0 \text{ in } Q_0, \quad \omega_\infty^{h'} \to \omega_\infty^0 \text{ in } V_T, \quad w_{i,\infty}^{h'} \to w_{i,\infty}^0 \text{ in } V_T, \ 1 \le i \le i_0, \tag{5.3}$$

$$u_{ij,\infty}^{h'} \to u_{ij,\infty}^0 \text{ in } V, \quad 1 \le i \le i_0, \ 1 \le j \le j_0, \tag{5.4}$$

where $u_{ij,\infty}^{h'} = u_j^{h'}(p_\infty^{h'}, \omega_\infty^{h'}, w_{i,\infty}^{h'})$, $u_{ij,\infty}^0 = u_j(p_\infty^0, \omega_\infty^0, w_{i,\infty}^0)$. *Moreover,* $(p_\infty^0, \omega_\infty^0, \boldsymbol{w}_\infty^0)$ *is a solution of Problem* 3.1.

Proof We first notice that $\|p_\infty^h\|_{Q_0}$, $\|\omega_\infty^h\|_{V_T}$, $\|w_{i,\infty}^h\|_{V_T}$ for $1 \le i \le i_0$, and $\|u_{ij,\infty}^h\|_{V_T}$ for $1 \le i \le i_0$, $1 \le j \le j_0$, are all uniformly bounded, independent of h. Thus for a subsequence $\{h' = (h'_\Omega, h'_{\Omega_0}, h'_T\ )\}$ of $\{h\}$, an element $(p_\infty^0, \omega_\infty^0, \boldsymbol{w}_\infty^0) \in \boldsymbol{Q}_{ad}^h$ and functions $u_{ij,\infty}^0 \in V$, $1 \le i \le i_0$, $1 \le j \le j_0$, such that as $h' \to 0$,

$$p_\infty^{h'} \rightharpoonup p_\infty^0 \text{ in } Q_0, \tag{5.5}$$

$$\omega_\infty^{h'} \rightharpoonup \omega_\infty^0 \text{ in } V_T, \quad \omega_\infty^{h'} \to \omega_\infty^0 \text{ in } C(\overline{I_T}), \tag{5.6}$$

$$w_{i,\infty}^{h'} \rightharpoonup w_{i,\infty}^0 \text{ in } V_T, \quad w_{i,\infty}^{h'} \to w_{i,\infty}^0 \text{ in } C(\overline{I_T}), \quad 1 \le i \le i_0, \tag{5.7}$$

$$u_{ij,\infty}^{h'} \rightharpoonup u_{ij,\infty}^0 \text{ in } V, \quad u_{ij,\infty}^{h'} \to u_{ij,\infty}^0 \text{ in } Q_\Gamma, \quad 1 \le i \le i_0, \ 1 \le j \le j_0. \tag{5.8}$$

Similar to the proof of Theorem 4.1, we can verify that $u_{ij,\infty}^0 = u_j(p_\infty^0, \omega_\infty^0, w_{i,\infty}^0)$ and

$$\begin{aligned} J(p_\infty^0, \omega_\infty^0, \boldsymbol{w}_\infty^0) &\le \liminf_{h' \to 0} J^{h'}(p_\infty^{h'}, \omega_\infty^{h'}, \boldsymbol{w}_\infty^{h'}) \\ &= \liminf_{h' \to 0} \inf_{(p^{h'}, \omega^{h'}, \boldsymbol{w}^{h'}) \in \boldsymbol{Q}_{ad}^{h'}} J^{h'}(p^{h'}, \omega^{h'}, \boldsymbol{w}^{h'}). \end{aligned} \tag{5.9}$$

Now let $(p, \omega, \boldsymbol{w}) \in \boldsymbol{Q}_{ad}$ be a solution of Problem 3.1 and let $u_{ij} = u_j(p, \omega, w_i)$ be defined by (3.1). Let $\Pi^{h_{\Omega_0}} p \in Q_0^{h_{\Omega_0}}$ be the piecewise average of p, $I^{h_T}\omega \in V_T^{h_T}$ and $I^{h_T} w_i \in V_T^{h_T}$ be the continuous piecewise linear interpolants of ω and w_i. Then by the finite element theory [22],

$$\|\Pi^{h_{\Omega_0}} p - p\|_{Q_0} \to 0, \ \|I^{h_T}\omega - \omega\|_{V_T} \to 0, \ \|I^{h_T} w_i - w_i\|_{V_T} \to 0, \text{ as } h \to 0. \tag{5.10}$$

Define $u_{ij}^h \in V^{h_\Omega}$ by

$$\begin{aligned} &\int_\Omega \left(D\nabla u_{ij}^h \cdot \nabla v^h + \mu u_{ij}^h v^h \right) \mathrm{d}x + \int_\Gamma \frac{1}{2A} u_{ij}^h v^h \, \mathrm{d}s \\ &\quad = \int_{\Omega_0} I^{h_T}\omega(T_j) \, I^{h_T} w_i(T_j) \, \Pi^{h_{\Omega_0}} p v^h \, \mathrm{d}x \quad \forall v^h \in V^{h_\Omega}. \end{aligned} \tag{5.11}$$

Then from the definitions (3.1) and (5.11), we can derive the following inequality:

$$\|u_{ij}-u_{ij}^h\|_V \le c\left[\inf_{v^{h_\Omega}\in V^{h_\Omega}} \|u_{ij}-v^{h_\Omega}\|_V + \|\omega(T_j)\,w_i(T_j)\,p - I^{h_T}\omega(T_j)\,I^{h_T}w_i(T_j)\,\Pi^{h_{\Omega_0}}p\|_{Q_0}\right]. \tag{5.12}$$

Because of the uniform boundedness of $\|I^{h_T}\omega\|_{C(\overline{I_T})}$, $\|I^{h_T}w_i\|_{C(\overline{I_T})}$ and $\|\Pi^{h_{\Omega 0}}p\|_{Q_0}$, we deduce from (5.12) that

$$\|u_{ij}-u_{ij}^h\|_V \le c\left[\inf_{v^{h_\Omega}\in V^{h_\Omega}} \|u_{ij}-v^{h_\Omega}\|_V + \|\omega - I^{h_T}\omega\|_{C(\overline{I_T})} + \|w_i - I^{h_T}w_i\|_{C(\overline{I_T})} + \|p-\Pi^{h_{\Omega_0}}p\|_{Q_0}\right].$$

In particular, this implies

$$\|u_{ij}-u_{ij}^h\|_V \to 0 \quad \text{as } h\to 0.$$

Thus,

$$\inf_{(p^h,\omega^h,\boldsymbol{w}^h)\in \boldsymbol{Q}_{ad}^h} J^h(p^h,\omega^h,\boldsymbol{w}^h) \le J^h(\Pi^{h_{\Omega_0}}p, I^{h_T}\omega, I^{h_T}\boldsymbol{w}) \to J(p,\omega,\boldsymbol{w}) \quad \text{as } h\to 0.$$

Therefore,

$$\limsup_{h'\to 0}\ \inf_{(p^{h'},\omega^{h'},\boldsymbol{w}^{h'})\in \boldsymbol{Q}_{ad}^{h'}} J^{h'}(p^{h'},\omega^{h'},\boldsymbol{w}^{h'}) \le J(p,\omega,\boldsymbol{w}). \tag{5.13}$$

Combining (5.9) and (5.13), we deduce that

$$J(p_\infty^0,\omega_\infty^0,\boldsymbol{w}_\infty^0) = \lim_{h'\to 0} J^{h'}(p_\infty^{h'},\omega_\infty^{h'},\boldsymbol{w}_\infty^{h'}) = J(p,\omega,\boldsymbol{w}).$$

So $(p_\infty^0,\omega_\infty^0,\boldsymbol{w}_\infty^0)$ is a solution of Problem 3.1, and as $h'\to 0$,

$$\|p_\infty^{h'}\|_{Q_0}\to\|p_\infty^0\|_{Q_0},\quad \|\omega_\infty^{h'}-\omega^{(0)}\|_{V_T}\to\|\omega_\infty^0-\omega^{(0)}\|_{V_T},$$
$$\|w_{i,\infty}^{h'}-w_i^{(0)}\|_{V_T}\to\|w_{i,\infty}^0-w_i^{(0)}\|_{V_T},\quad 1\le i\le i_0.$$

These relations and the weak convergence of (5.5)–(5.7) together imply the strong convergence in (5.3) [20]. To show the strong convergence (5.4), we use the definitions (3.1) and (5.1) and write

$$\begin{aligned}
&\int_\Omega\left[D\,|\nabla(u_{ij,\infty}^{h'}-u_{ij,\infty}^0)|^2+\mu\,|u_{ij,\infty}^{h'}-u_{ij,\infty}^0|^2\right]\mathrm{d}x+\int_\Gamma\frac{1}{2A}|u_{ij,\infty}^{h'}-u_{ij,\infty}^0|^2\,\mathrm{d}s\\
&\quad=\int_{\Omega_0}\left[\omega_\infty^{h'}(T_j)\,w_{i,\infty}^{h'}(T_j)\,p_\infty^{h'}-\omega_\infty^0(T_j)\,w_{i,\infty}^0(T_j)\,p_\infty^0\right]u_{ij,\infty}^{h'}\,\mathrm{d}x\\
&\qquad+\int_{\Omega_0}\omega_\infty^0(T_j)\,w_{i,\infty}^0(T_j)\,p_\infty^0\left(u_{ij,\infty}^{h'}-u_{ij,\infty}^0\right)\mathrm{d}x+\int_\Gamma\frac{1}{A}u_{ij,\infty}^0(u_{ij,\infty}^0-u_{ij,\infty}^{h'})\mathrm{d}s\\
&\qquad+2\int_\Omega\left[D\nabla u_{ij,\infty}^0\cdot\nabla(u_{ij,\infty}^0-u_{ij,\infty}^{h'})+\mu u_{ij,\infty}^0(u_{ij,\infty}^0-u_{ij,\infty}^{h'})\right]\mathrm{d}x.
\end{aligned}$$

As $h'\to 0$, the first term on the right side approaches zero because of the boundedness of $\{\|u_{ij,\infty}^{h'}\|_{L^2(\Omega_0)}\}_{h'}$ and the strong convergence $\omega_\infty^{h'}\to\omega_\infty^0$ and

$w_{i,\infty}^{h'} \to w_{i,\infty}^{0}$ in V_T, $p_{\infty}^{h'} \to p_{\infty}^{0}$ in Q_0. The other terms approach zero because of the convergence property (5.8). Thus,

$$\int_{\Omega}\Big[D\,|\nabla(u_{ij,\infty}^{h'} - u_{ij,\infty}^{0})|^2 + \mu\,|u_{ij,\infty}^{h'} - u_{ij,\infty}^{0}|^2\Big]\mathrm{d}x + \int_{\Gamma}\frac{1}{2A}|u_{ij,\infty}^{h'} - u_{ij,\infty}^{0}|^2\,\mathrm{d}s \to 0 \quad \text{as } h' \to 0.$$

So we have the strong convergence (5.4). ■

6. An iterative scheme based on linearization

The discussion in the section is made at the continuous level, i.e. for Problem 3.1. All the results can be extended to the discrete Problem 5.1 in a straightforward fashion.

Note that Problem 3.1 has three unknowns p, ω and $\boldsymbol{w}$, but approximate values $\omega^{(0)}$ and $\boldsymbol{w}^{(0)}$ of ω and $\boldsymbol{w}$ are available from prior experiments. We may first determine an approximate value $p^{(0)}$ for p and then develop an iterative scheme based on the idea of linearization.

First we compute $p^{(0)}$. Consider Problem 3.1 with freezed $\omega = \omega^{(0)}$ and $\boldsymbol{w} = \boldsymbol{w}^{(0)}$. In other words, we consider the following problem.

Problem 6.1 Find $p \in Q_p$ such that the objective functional $J(p, \omega^{(0)}, \boldsymbol{w}^{(0)})$ is minimal over Q_p.

This problem is similar to the standard BLT/MBT problems studied in the literature, [10,16]. There is a unique solution $p^{(0)} \in Q_p$, which is characterized by an inequality

$$\sum_{i,j}\Big(u_{ij}^{(0)}(p^{(0)}) - f_{ij}, u_{ij}^{(0)}(p) - u_{ij}^{(0)}(p^{(0)})\Big)_{Q_{\Gamma_i}} + \varepsilon\big(p^{(0)}, p - p^{(0)}\big)_{Q_0} \geq 0 \quad \forall p \in Q_p.$$

Here $u_{ij}^{(0)}(p) \in V$ is defined by a boundary value problem:

$$\int_{\Omega}\Big(D\nabla u_{ij}^{(0)}(p)\cdot\nabla v + \mu u_{ij}^{(0)}(p)v\Big)\mathrm{d}x + \int_{\Gamma}\frac{1}{2A}u_{ij}^{(0)}(p)v\,\mathrm{d}s = \int_{\Omega_0}\omega^{(0)}(T_j)\,w_i^{(0)}(T_j)pv\,\mathrm{d}x \quad \forall v \in V.$$

Let us discuss the idea of linearization. Write

$$p = p^{(0)} + \delta_p, \quad \omega = \omega^{(0)} + \delta_\omega, \quad \boldsymbol{w} = \boldsymbol{w}^{(0)} + \boldsymbol{\delta}_w.$$

Here $\boldsymbol{\delta}_w = (\delta_{w_1}, \ldots, \delta_{w_{i0}})^T$. These δ terms are expected to be small, and we drop terms of second or higher orders of these to obtain

$$\omega(T_j)\,w_i(T_j)\,p \approx \omega^{(0)}(T_j)\,w_i^{(0)}(T_j)\,p^{(0)} + \omega^{(0)}(T_j)\,w_i^{(0)}(T_j)\,\delta_p + w_i^{(0)}(T_j)\,p^{(0)}\delta_\omega(T_j) + \omega^{(0)}(T_j)\,p^{(0)}\delta_{w_i}(T_j).$$

Then the solution $u_j(p, \omega, w_i)$ of the problem (3.1) satisfies

$$u_j(p, \omega, w_i) \approx u_{ij}^{(0)}(p^{(0)}) + \delta_{u,ij},$$

where we define $\delta_{u,ij} \in V$ by

$$\int_\Omega \big(D\nabla\delta_{u,ij}\cdot\nabla v+\mu\delta_{u,ij}v\big)\mathrm{d}x+\int_\Gamma \frac{1}{2A}\delta_{u,ij}v\,\mathrm{d}s$$
$$=\int_{\Omega_0}\Big[\omega^{(0)}(T_j)\,w_i^{(0)}(T_j)\,\delta_p+w_i^{(0)}(T_j)\,p^{(0)}\delta_\omega(T_j)+\omega^{(0)}(T_j)\,p^{(0)}\delta_{w_i}(T_j)\Big]v\,\mathrm{d}x\quad \forall v\in V.$$

Based on the above discussion, we propose the following iterative scheme.

For $k=0,1,\ldots$, with $(p^{(k)},\omega^{(k)},\boldsymbol{w}^{(k)})\in\boldsymbol{Q}_{ad}$ known, define $u_{ij}^{(k)}\in V$ by the problem

$$\int_\Omega\Big(D\nabla u_{ij}^{(k)}\cdot\nabla v+\mu u_{ij}^{(k)}v\Big)\mathrm{d}x+\int_\Gamma\frac{1}{2A}u_{ij}^{(k)}v\,\mathrm{d}s=\int_{\Omega_0}\omega^{(k)}(T_j)\,w_i^{(k)}(T_j)\,p^{(k)}v\,\mathrm{d}x\quad\forall v\in V. \tag{6.1}$$

Define

$$\boldsymbol{Q}_{ad}^{(k)}=\big\{(\delta_p,\delta_\omega,\boldsymbol{\delta}_w)\in Q_0\times V_T\times(V_T)^{i_0}\mid(p^{(k)}+\delta_p,\omega^{(k)}+\delta_\omega,\boldsymbol{w}^{(k)}+\boldsymbol{\delta}_w)\in\boldsymbol{Q}_{ad}\big\}.$$

It is easy to show that $\boldsymbol{Q}_{ad}^{(k)}$ is a non-empty, closed, convex set in the space $Q_0\times V_T\times(V_T)^{i_0}$. For $(\delta_p,\delta_\omega,\boldsymbol{\delta}_w)\in\boldsymbol{Q}_{ad}^{(k)}$, define $\delta_{u,ij}\in V$ by

$$\int_\Omega\big(D\nabla\delta_{u,ij}\cdot\nabla v+\mu\delta_{u,ij}v\big)\mathrm{d}x+\int_\Gamma\frac{1}{2A}\delta_{u,ij}v\,\mathrm{d}s$$
$$=\int_{\Omega_0}\Big[\omega^{(k)}(T_j)\,w_i^{(k)}(T_j)\,\delta_p+w_i^{(k)}(T_j)\,p^{(k)}\delta_\omega(T_j)+\omega^{(k)}(T_j)\,p^{(k)}\delta_{w_i}(T_j)\Big]v\,\mathrm{d}x\quad\forall v\in V, \tag{6.2}$$

and introduce the functional

$$J_\delta^{(k)}(\delta_p,\delta_\omega,\boldsymbol{\delta}_w)=\frac{1}{2}\sum_{i,j}\|u_{ij}^{(k)}+\delta_{u,ij}-f_{ij}\|_{Q_{\Gamma_i}}^2+\frac{\varepsilon}{2}\|\delta_p\|_{Q_0}^2$$
$$+\frac{M_\omega}{2}\|\delta_\omega\|_{V_T}^2+\frac{M_w}{2}\sum_i\|\delta_{w_i}\|_{V_T}^2. \tag{6.3}$$

We determine $(\delta_p^{(k)},\delta_\omega^{(k)},\boldsymbol{\delta}_w^{(k)})$ from the following problem.

Problem 6.2 *Find* $(\delta_p^{(k)},\delta_\omega^{(k)},\boldsymbol{\delta}_w^{(k)})\in\boldsymbol{Q}_{ad}^{(k)}$ *that minimizes the functional* $J^{(k)}(\delta_p,\delta_\omega,\boldsymbol{\delta}_w)$ *over* $\boldsymbol{Q}_{ad}^{(k)}$.

As output of the iteration step, we let

$$p^{(k+1)}=p^{(k)}+\delta_p^{(k)},\quad\omega^{(k+1)}=\omega^{(k)}+\delta_\omega^{(k)},\quad\boldsymbol{w}^{(k+1)}=\boldsymbol{w}^{(k)}+\boldsymbol{\delta}_w^{(k)}. \tag{6.4}$$

Regarding Problem 6.2, we have the following result.

Theorem 6.3 *Problem* 6.2 *has a unique solution* $(\delta_p^{(k)},\delta_\omega^{(k)},\boldsymbol{\delta}_w^{(k)})\in\boldsymbol{Q}_{ad}^{(k)}$, *which is characterized by an inequality*

$$\sum_{i,j}\Big(u_{ij}^{(k)}+\delta_{u,ij}^{(k)}-f_{ij},\delta_{u,ij}-\delta_{u,ij}^{(k)}\Big)_{Q_{\Gamma_i}}+\varepsilon\Big(\delta_p^{(k)},\delta_p-\delta_p^{(k)}\Big)_{Q_0}$$
$$+M_\omega\big(\delta_\omega^{(k)},\delta_\omega-\delta_\omega^{(k)}\big)_{V_T}+M_w\sum_i\Big(\delta_{w_i}^{(k)},\delta_{w_i}-\delta_{w_i}^{(k)}\Big)_{V_T}\ge 0\quad\forall(\delta_p,\delta_\omega,\boldsymbol{\delta}_w)\in\boldsymbol{Q}_{ad}^{(k)}, \tag{6.5}$$

where $u_{ij}^{(k)} \in V$ *is defined by* (6.1), $\delta_{u,ij} \in V$ *is defined by* (6.2) *and* $\delta_{u,ij}^{(k)} \in V$ *is defined by*

$$\int_\Omega \Big(D\nabla\delta_{u,ij}^{(k)} \cdot \nabla v + \mu\delta_{u,ij}^{(k)} v \Big) \mathrm{d}x + \int_\Gamma \frac{1}{2A}\delta_{u,ij} v \, \mathrm{d}s$$
$$= \int_{\Omega_0} \Big[\omega^{(k)}(T_j)\, w_i^{(k)}(T_j)\, \delta_p^{(k)} + w_i^{(k)}(T_j)\, p^{(k)} \delta_\omega^{(k)}(T_j) + \omega^{(k)}(T_j)\, p^{(k)} \delta_{w_i}^{(k)}(T_j) \Big] v \, \mathrm{d}x \quad \forall v \in V.$$

Numerical methods for Problem 6.2 can be similarly developed, and convergence of the numerical solutions can be shown.

7. Limiting behaviours

We first consider the limiting behaviour of the solution of Problem 3.1 as $M_\omega \to \infty$. Let $\boldsymbol{Q}_{ad}^{(1)} = Q_p \times \boldsymbol{Q}_w$. Then $\boldsymbol{Q}_{ad}^{(1)}$ is a non-empty, closed, convex set in the space $Q_0 \times (V_T)^{i_0}$. For any $(p, \boldsymbol{w}) \in \boldsymbol{Q}_{ad}^{(1)}$, we define $u_{ij}^{(1)} = u_j^{(1)}(p, w_i) \in V$ by

$$\int_\Omega \Big(D\nabla u_{ij}^{(1)} \cdot \nabla v + \mu u_{ij}^{(1)} v \Big) \mathrm{d}x + \int_\Gamma \frac{1}{2A} u_{ij}^{(1)} v \, \mathrm{d}s = \int_{\Omega_0} \omega^{(0)}(T_j)\, w_i(T_j)\, pv \, \mathrm{d}x \quad \forall v \in V \tag{7.1}$$

for $1 \le i \le i_0$, $1 \le j \le j_0$. By the assumptions made on the data D, μ and A, it follows from an application of the Lax–Milgram lemma that the solution $u_{ij}^{(1)}$ is uniquely defined by (7.1). For positive numbers ε and M_w, we introduce the objective functional

$$J^{(1)}(p, \boldsymbol{w}) = \frac{1}{2}\sum_{i,j} \| u_j^{(1)}(p, w_i) - f_{ij} \|_{Q_{\Gamma_i}}^2 + \frac{\varepsilon}{2}\|p\|_{Q_0}^2 + \frac{M_w}{2}\sum_i \|w_i - w_i^{(0)}\|_{V_T}^2 \tag{7.2}$$

and the following problem.

Problem 7.1 *Find* $(p, \boldsymbol{w}) \in \boldsymbol{Q}_{ad}^{(1)}$ *such that the objective functional* $J^{(1)}(p, \boldsymbol{w})$ *is minimal over* $\boldsymbol{Q}_{ad}^{(1)}$.

Notice that Problem 7.1 is a degenerate case of Problem 3.1 when Q_ω is replaced by a one element set $\{\omega^{(0)}\}$. In other words, we study Problem 7.1 when $\omega^{(0)}$ is known to be the exact normalized total energy function.

Similar to Theorem 4.1, we can show Problem 7.1 has a solution. Our focus here is on relationship between Problem 3.1 and Problem 7.1.

Theorem 7.2 *Let* $(p_n, \omega_n, \boldsymbol{w}_n) \in \boldsymbol{Q}_{ad}$ *be a solution of Problem* 3.1 *for* $M_\omega = M_n$ *with* $M_n \to \infty$ *as* $n \to \infty$. *Then*

$$\omega_n \to \omega^{(0)} \text{ in } V_T \quad \text{as } n \to \infty, \tag{7.3}$$

and there exist a subsequence $\{n'\}$ *of the sequence* $\{n\}$ *and a solution* $(p_\infty^{(1)}, \boldsymbol{w}_\infty^{(1)}) \in \boldsymbol{Q}_{ad}^{(1)}$ *of Problem* 7.1 *such that as* $n' \to \infty$,

$$p_{n'} \to p_\infty^{(1)} \text{ in } Q_0, \quad w_{i,n'} \to w_{i,\infty}^{(1)} \text{ in } V_T,\ 1 \le i \le i_0, \tag{7.4}$$

$$u_{ij,n'} \to u_{ij,\infty}^{(1)} \text{ in } V,\ 1 \le i \le i_0,\ 1 \le j \le j_0, \tag{7.5}$$

where $u_{ij,n'} = u_j(p_{n'}, \omega_{n'}, w_{i,n'})$, $u_{ij,\infty}^{(1)} = u_j^{(1)}(p_\infty^{(1)}, w_{i,\infty}^{(1)})$.

Proof To stress the dependence of the functional $J(\cdot,\cdot,\cdot)$ of (3.2) on $M_\omega = M_n$, we write it as $J_n(\cdot,\cdot,\cdot)$ in this proof. Let $(p_\infty, \boldsymbol{w}_\infty) \in \boldsymbol{Q}_{ad}^{(1)}$ be a solution of Problem 7.1. Then

$$J_n(p_n, \omega_n, \boldsymbol{w}_n) \le J_n(p_\infty, \omega^{(0)}, \boldsymbol{w}_\infty) = J^{(1)}(p_\infty, \boldsymbol{w}_\infty). \tag{7.6}$$

In particular, this implies $\omega_n \to \omega^{(0)}$ in V_T. So (7.3) holds. Notice that $\|p_n\|_{Q_0}$, $\|w_{i,n}\|_{V_T}$ and $\|u_{ij,n}\|_V$, $1 \le i \le i_0$, $1 \le j \le j_0$, are uniformly bounded. Hence, there exist a subsequence $\{(p_{n'}, \boldsymbol{w}_{n'})\}$, an element $(p_\infty^{(1)}, \boldsymbol{w}_\infty^{(1)}) \in Q_{ad}^{(1)}$ and $u_{ij,\infty}^{(1)} \in V$, $1 \le i \le i_0$, $1 \le j \le j_0$, such that

$$p_{n'} \rightharpoonup p_\infty^{(1)} \text{ in } Q_0, \tag{7.7}$$

$$w_{i,n'} \rightharpoonup w_{i,\infty}^{(1)} \text{ in } V_T, \quad w_{i,n'} \to w_{i,\infty}^{(1)} \text{ in } C(\overline{I_T}),\ 1 \le i \le i_0, \tag{7.8}$$

$$u_{ij,n'} \rightharpoonup u_{ij,\infty}^{(1)} \text{ in } V, \quad u_{ij,n'} \to u_{ij,\infty}^{(1)} \text{ in } Q_\Gamma,\ 1 \le i \le i_0,\ 1 \le j \le j_0, \tag{7.9}$$

We need to show

(a) $u_{ij,\infty}^{(1)} = u_j^{(1)}(p_\infty^{(1)}, w_{i,\infty}^{(1)})$;
(b) $(p_\infty^{(1)}, \boldsymbol{w}_\infty^{(1)})$ is a solution of Problem 7.1;
(c) strong convergence (7.4) and (7.5).

It is easy to see that (a) is valid. For (b) and (c), we first deduce the following inequality from (7.6):

$$\limsup_{n\to\infty} J_n(p_n, \omega_n, \boldsymbol{w}_n) \le J^{(1)}(p_\infty, \boldsymbol{w}_\infty). \tag{7.10}$$

Then we have the following sequence of inequalities:

$$\begin{aligned}
J^{(1)}(p_\infty^{(1)}, \boldsymbol{w}_\infty^{(1)}) &\le \liminf_{n'\to\infty} J^{(1)}(p_{n'}, \boldsymbol{w}_{n'}) \\
&\le \limsup_{n'\to\infty} J^{(1)}(p_{n'}, \boldsymbol{w}_{n'}) \\
&= \limsup_{n'\to\infty} \left[J_{n'}(p_{n'}, \omega_{n'}, \boldsymbol{w}_{n'}) - \frac{M_{n'}}{2} \|\omega_{n'} - \omega^{(0)}\|_{V_T}^2 \right] \\
&\le \limsup_{n'\to\infty} J_{n'}(p_{n'}, \omega_{n'}, \boldsymbol{w}_{n'}) \\
&\le J^{(1)}(p_\infty, \boldsymbol{w}_\infty)
\end{aligned}$$

where in the last step, we used (7.10). So $(p_\infty^{(1)}, \boldsymbol{w}_\infty^{(1)})$ is a solution of Problem 7.1 and

$$\lim_{n'\to\infty} J^{(1)}(p_{n'}, \boldsymbol{w}_{n'}) = J^{(1)}(p_\infty^{(1)}, \boldsymbol{w}_\infty^{(1)}).$$

Taking (7.7)–(7.9) into consideration, the equality implies that as $n' \to \infty$,

$$\|p_{n'}\|_{Q_0} \to \|p_\infty^{(1)}\|_{Q_0}, \quad \|w_{i,n'}^{(1)}\|_{V_T} \to \|w_{i,\infty}^{(1)}\|_{V_T},\ 1 \le i \le i_0.$$

The above norm sequence convergence and the weak convergence property (7.7) and (7.8) together imply the strong convergence (7.4). Proof of the strong convergence (7.5) is similar to that of (5.4). ■

From the proof of the theorem, we find that

$$\lim_{n'\to\infty} M_{n'}\|\omega_{n'} - \omega^{(0)}\|_{V_T}^2 = 0.$$

This relation indicates that the speed with which $\omega_{n'}$ converges to $\omega^{(0)}$ in V_T is faster than that with which $1/\sqrt{M_{n'}}$ converges to zero.

We then consider the limiting behaviour of the solution of Problem 3.1 as $M_w \to \infty$. Let $\boldsymbol{Q}_{ad}^{(2)} = Q_p \times Q_\omega$. Then $\boldsymbol{Q}_{ad}^{(2)}$ is a non-empty, closed, convex set in the space $Q_0 \times V_T$. For any $(p,\omega) \in \boldsymbol{Q}_{ad}^{(2)}$, we define $u_{ij}^{(2)} = u_{ij}^{(2)}(p,\omega) \in V$ by

$$\int_\Omega \Big(D\nabla u_{ij}^{(2)} \cdot \nabla v + \mu u_{ij}^{(2)} v\Big)\mathrm{d}x + \int_\Gamma \frac{1}{2A} u_{ij}^{(2)} v \,\mathrm{d}s = \int_{\Omega_0} \omega(T_j)\, w_i^{(0)}(T_j)\, pv\,\mathrm{d}x \quad \forall v \in V \tag{7.11}$$

for $1 \le i \le i_0$, $1 \le j \le j_0$. By the assumptions made on the data D, μ and A, it follows from an application of the Lax–Milgram lemma that the solution $u_{ij}^{(2)}$ is uniquely defined by (7.11). For positive numbers ε and M_ω, we introduce the objective functional

$$J^{(2)}(p,\boldsymbol{w}) = \frac{1}{2}\sum_{i,j} \|u_{ij}^{(2)}(p,\omega) - f_{ij}\|_{Q_{\Gamma_i}}^2 + \frac{\varepsilon}{2}\|p\|_{Q_0}^2 + \frac{M_\omega}{2}\|\omega - \omega^{(0)}\|_{V_T}^2 \tag{7.12}$$

and the following problem.

Problem 7.3 *Find* $(p,\omega) \in \boldsymbol{Q}_{ad}^{(2)}$ *such that the objective functional* $J^{(2)}(p,\omega)$ *is minimal over* $\boldsymbol{Q}_{ad}^{(2)}$.

Notice that Problem 7.3 is a degenerate case of Problem 3.1 when $\boldsymbol{Q}_w$ is replaced by a one element set $\{\boldsymbol{w}^{(0)}\}$. In other words, we study Problem 7.3 when $\boldsymbol{w}^{(0)}$ is known to be the exact multispectral energy percentage vector function.

We can show that Problem 7.3 has a solution. Similar to Theorem 7.2, we have the next result regarding Problem 7.3.

Theorem 7.4 *Let* $(p_n, \omega_n, \boldsymbol{w}_n) \in \boldsymbol{Q}_{ad}$ *be a solution of Problem* 3.1 *for* $M_w = M_n$ *with* $M_n \to \infty$ *as* $n \to \infty$. *Then*

$$w_{i,n} \to w_i^{(0)} \text{ in } V_T \text{ as } n \to \infty, \quad 1 \le i \le i_0,$$

and there exist a subsequence $\{n'\}$ *of* $\{n\}$ *and a solution* $(p_\infty^{(2)}, \omega_\infty^{(2)}) \in \boldsymbol{Q}_{ad}^{(2)}$ *of Problem* 7.3 *such that as* $n' \to \infty$,

$$p_{n'} \to p_\infty^{(2)} \text{ in } Q_0, \quad \omega_{n'} \to \omega_\infty^{(2)} \text{ in } V_T,$$

$$u_{ij,n'} \to u_{ij,\infty}^{(2)} \text{ in } V, \quad 1 \le i \le i_0,\ 1 \le j \le j_0,$$

where $u_{ij,n'} = u_j(p_{n'}, \omega_{n'}, w_{i,n'})$, $u_{ij,\infty}^{(2)} = u_{ij}^{(2)}(p_\infty^{(2)}, \omega_\infty^{(2)})$.

It is easy to extend the above discussion to the situation where only some of the energy percentage functions are known exactly. Let $I \subset \{1,\ldots,i_0\}$ be the index set for those energy percentage functions that are not known exactly.

Define $\tilde{\boldsymbol{Q}}_{ad} = Q_p \times Q_\omega \times \tilde{\boldsymbol{Q}}_{w,I}$ where $\tilde{\boldsymbol{Q}}_{w,I} = \{\boldsymbol{w} \in \boldsymbol{Q}_w \mid w_i = w_i^{(0)}\ \forall i \notin I\}$. Then $\tilde{\boldsymbol{Q}}_{ad}$ is a non-empty, closed, convex set in the space $Q_0 \times V_T \times (V_T)^{i_0}$. Modify (3.2) to

$$\tilde{J}(p,\omega,\boldsymbol{w}) = \frac{1}{2}\sum_j \left[\sum_{i\in I} \|u_j(p,\omega,w_i) - f_{ij}\|^2_{Q_{\Gamma_i}} + \sum_{i\notin I} \|u_j(p,\omega,w_i^{(0)}) - f_{ij}\|^2_{Q_{\Gamma_i}} \right] + \frac{\varepsilon}{2}\|p\|^2_{Q_0} + \frac{M_\omega}{2}\|\omega - \omega^{(0)}\|^2_{V_T} + \frac{M_w}{2}\sum_{i\in I}\|w_i - w_i^{(0)}\|^2_{V_T},$$

and then minimize $\tilde{J}(p,\omega,\boldsymbol{w})$ over the set $\tilde{\boldsymbol{Q}}_{ad}$. Similar theoretical results hold for this problem.

We can also consider the limiting behaviour of the solution of Problem 3.1 as both $M_\omega \to \infty$ and $M_w \to \infty$. Let $Q_{ad}^{(3)} = Q_p$. Then $Q_{ad}^{(3)}$ is a non-empty, closed, convex set in the space Q_0. For any $p \in Q_{ad}^{(3)}$, we define $u_{ij}^{(3)} = u_{ij}^{(3)}(p) \in V$ by

$$\int_\Omega \left(D\nabla u_{ij}^{(3)} \cdot \nabla v + \mu u_{ij}^{(3)} v \right) \mathrm{d}x + \int_\Gamma \frac{1}{2A} u_{ij}^{(3)} v \,\mathrm{d}s = \int_{\Omega_0} \omega^{(0)}(T_j)\, w_i^{(0)}(T_j)\, pv \,\mathrm{d}x \quad \forall v \in V \tag{7.13}$$

for $1 \le i \le i_0$, $1 \le j \le j_0$. By the assumptions made on the data D, μ and A, it follows from an application of the Lax–Milgram lemma that the solution $u_{ij}^{(3)}$ is uniquely defined by (7.13). For a positive number ε, we introduce the objective functional

$$J^{(3)}(p) = \frac{1}{2}\sum_{i,j} \|u_{ij}^{(3)}(p) - f_{ij}\|^2_{Q_{\Gamma_i}} + \frac{\varepsilon}{2}\|p\|^2_{Q_0} \tag{7.14}$$

and the following problem:

PROBLEM 7.5 *Find $p \in Q_{ad}^{(3)}$ such that the objective functional $J^{(3)}(p)$ is minimal over $Q_{ad}^{(3)}$.*

Notice that Problem 7.5 is a degenerate case of Problem 3.1 when Q_ω is replaced by a one element set $\{\omega^{(0)}\}$ and $\boldsymbol{Q}_w$ is replaced by $\{\boldsymbol{w}^{(0)}\}$. In other words, Problem 7.5 is intended for the situation where both the normalized total energy function and multispectral energy percentage vector function are known exactly.

We can show this problem has a solution. Similar to Theorems 7.2 and 7.4, we have the following result on Problem 7.5.

THEOREM 7.6 *Let $(p_n, \omega_n, \boldsymbol{w}_n) \in \boldsymbol{Q}_{ad}$ be a solution of Problem 3.1 for $M_\omega = M_{2,n}$ and $M_w = M_{3,n}$, with $M_{2,n} \to \infty$ and $M_{3,n} \to \infty$ as $n \to \infty$. Then as $n \to \infty$,*

$$\omega_n \to \omega^{(0)} \text{ in } V_T, \quad w_{i,n} \to w_i^{(0)} \text{ in } V_T,\ 1 \le i \le i_0.$$

Moreover, there exist a subsequence $\{n'\}$ of $\{n\}$ and a solution $p_\infty^{(3)} \in Q_{ad}^{(3)}$ of Problem 7.5 such that as $n' \to \infty$,

$$p_{n'} \to p_\infty^{(3)} \quad \text{in } Q_0,$$
$$u_{ij,n'} \to u_{ij,\infty}^{(3)} \quad \text{in } V,\ 1 \le i \le i_0,\ 1 \le j \le j_0,$$

where $u_{ij,n'} = u_j(p_{n'}, \omega_{n'}, w_{i,n'})$, $u_{ij,\infty}^{(3)} = u_{ij}^{(3)}(p_\infty^{(3)})$.

8. Numerical examples

In this section, we report some numerical results to illustrate the usefulness of measurements from multiple temperature distributions in improving the accuracy of the reconstructed bioluminescent source distribution.

Example 8.1 We consider a two-dimensional domain $\Omega = (0, 1) \times (0, 1)$. The region $\overline{\Omega}$ is divided into four subregions $\overline{\Omega_m}$, $1 \le m \le 4$, with $\Omega_1 = (0, 0.5) \times (0, 0.5)$, $\Omega_2 = (0.5, 1) \times (0, 0.5)$, $\Omega_3 = (0, 0.5) \times (0.5, 1)$ and $\Omega_4 = (0.5, 1) \times (0.5, 1)$. In each subregion Ω_m, $1 \le m \le 4$, the values of the optical parameters D and μ are constant. The values of D in the four regions are 0.3268, 0.1916, 0.5464 and 0.2415, and the values of μ are 0.02, 0.14, 0.01 and 0.08, respectively. We choose $A = 1$. The source p is placed in the region $(0.25, 0.375) \times (0.125, 0.375)$ where the function value is 6. The permissible region is taken to be $\Omega_0 = (0.125, 0.375) \times (0.125, 0.375)$. We divide $\overline{\Omega_0}$ into eight congruent triangles and take the admissible set $Q_p^{h_{\Omega_0}}$ to consist of piecewise constant functions. The numbering of the eight triangles is shown in Figure 2.

We use constant temperature distribution T_j in each experiment j, $1 \le j \le 4$. The four temperature distributions used are $T_1 = 37°\mathrm{C}$, $T_2 = 39°\mathrm{C}$, $T_3 = 35°\mathrm{C}$ and $T_4 = 33°\mathrm{C}$. The corresponding exact values of normalized total energy function at these temperatures are $\omega = (1, 1.0509, 0.9414, 0.8771)^T$ and the exact energy percentage function values in the three spectral bands are

$$w_1 = (0.2844, 0.2598, 0.3095, 0.3364)^T,$$
$$w_2 = (0.3264, 0.3307, 0.3204, 0.3130)^T,$$
$$w_3 = (0.3892, 0.4095, 0.3701, 0.3506)^T.$$

We use linear elements on uniform triangular partitions of the domain Ω. The uniform meshes are obtained by dividing the interval $[0, 1]$ into $1/h$ equal parts in both x and y directions. We start with an initial mesh with $h = 1/8$ and then successively halve h to obtain more refined meshes. We take the numerical solutions of the BVP (3.1) computed using the exact values of p, ω and $\boldsymbol{w}$ and on the mesh with mesh size $h = 1/512$ as the true solution and use it to obtain the measured quantities

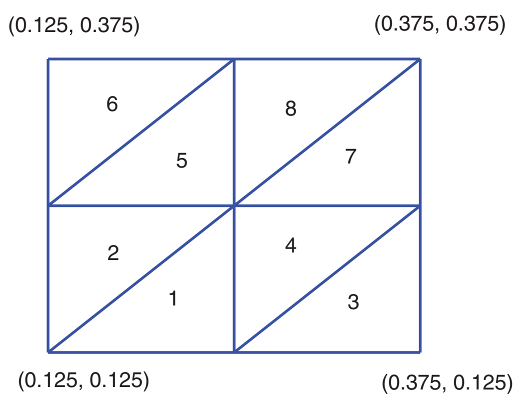

Figure 2. Numbering of the eight triangles for the permissible region.

f_{ij} on $\Gamma_i = \Gamma, 1 \leq i \leq 3, 1 \leq j \leq 4$. The numerical solutions of the problem (5.1) are then computed using these values of f_{ij} on the meshes with mesh size $h = 1/8, 1/16, 1/32$ using Matlab and its Optimization Toolbox.

We distinguish two cases. First, we assume the normalized total energy functions ω and the energy percentage function $\boldsymbol{w}$ to be known and reconstruct the unknown source function p from multi-spectral measurements of outgoing photon densities. Since the only unknown is p, we replace (5.2) by the following functional

$$J^h(p^h) = \frac{1}{2}\sum_{i,j} \|u_j^h(p^h) - f_{ij}\|^2_{Q_{\Gamma_i}} + \frac{\varepsilon}{2}\|p^h\|^2_{Q_0},$$

where $u_j^h(p^h)$ is determined by (5.1) with $\omega^h = \omega$ and $\boldsymbol{w}^h = \boldsymbol{w}$, and look for $p^h \in Q_p^{h\Omega_0}$ which minimizes this functional.

Using $\varepsilon = 10^{-5}$, we computed p^h using one ($T = T_1$) and four temperature distributions ($T = T_1, T_2, T_3, T_4$), respectively. The values of the reconstructed source function are respectively given in Tables 1 and 2. The last row in each table gives the values of the exact source function p. In these and later tables, an entry 0 for a numerical result represents the value 0 or a value of size $O(10^{-16})$.

Note that the total source power, i.e. the L^1 norm of the exact source p, is 0.1875. In Table 3, we list the reconstructed source powers for one and four

Table 1. Simulation results with one temperature distribution.

Element	1	2	3	4	5	6	7	8
p^h, $h = 1/8$	0.2107	0	6.9921	4.5387	1.7817	1.1067	5.3777	4.1501
p^h, $h = 1/16$	0.5458	0	7.3273	4.7643	1.4998	0.5741	5.4138	4.1343
p^h, $h = 1/32$	0.5939	0	6.8690	4.6132	1.5639	0.8177	5.2959	4.4156
p	0	0	6	6	0	0	6	6

Table 2. Simulation results with four temperature distributions.

Element	1	2	3	4	5	6	7	8
p^h, $h = 1/8$	0	0	7.4592	4.0390	0.9639	0.6044	6.1966	4.7526
p^h, $h = 1/16$	0	0	7.2504	4.3181	1.0064	0.1030	6.2447	5.1395
p^h, $h = 1/32$	0	0	6.8316	4.4831	1.2203	0.0437	6.2296	5.2080
p	0	0	6	6	0	0	6	6

Table 3. Reconstructed source powers.

h	1/8	1/16	1/32
One temperatures	0.1887	0.1895	0.1888
Four temperatures	0.1876	0.1880	0.1876

temperature distributions. Improvements gained through the use of measurements from four temperature distributions are evident.

Next, we only assume the approximate values of ω and $\boldsymbol{w}$ and reconstruct the source function p as well as ω and $\boldsymbol{w}$. We again perform the simulations using the one and four temperature distributions. The corresponding values of $\omega^{(0)}$ and $\boldsymbol{w}^{(0)}$ used are

$$\omega^{(0)} = (1.1, 1.2, 0.85, 0.80)^T,$$
$$w_1^{(0)} = (0.22, 0.3, 0.35, 0.4)^T,$$
$$w_2^{(0)} = (0.46, 0.4, 0.25, 0.38)^T,$$
$$w_3^{(0)} = (0.32, 0.3, 0.4, 0.22)^T.$$

We choose $\varepsilon = 10^{-4}$, $M_\omega = 10^{-2}$ and $M_w = 10^{-2}$.

In the first simulation we used only $T = T_1$, and in the second simulation we used all the four distributions in the reconstruction of the solution. Since we are using constant temperature distributions, the terms $\|\omega^h - \omega^{(0)}\|^2_{V_T}$ and $\sum_i \|w_i^h - w_i^{(0)}\|^2_{V_T}$ in functional (5.2) are replaced by $\sum_i |\omega_i^h - \omega_i^{(0)}|^2$ and $\sum_{i,j} |w_{ij}^h - w_{ij}^{(0)}|^2$, respectively, for computing the numerical solutions. We used the iterative scheme described in Section 6 to compute the solution performing only one iteration in all cases. Also we replace the terms $\|\delta_\omega\|^2_{V_T}$ and $\sum_i \|\delta_{w_i}\|^2_{V_T}$ in functional (6.3) by the corresponding sums to take account of the discrete temperature distributions used. Tables 4 and 5 give the computed values of p^h using one and four temperatures distributions, respectively.

Recall that the total source power of the exact source p is 0.1875. In Table 6, we list the reconstructed source powers for one and four temperature distributions. Again, we observe improvement due to the use of measurements for the four temperature distributions. ■

Table 4. Simulation results with one temperature distribution.

Element	1	2	3	4	5	6	7	8
p^h, $h = 1/8$	1.9775	1.4441	3.8885	3.1770	2.2500	1.9762	3.4490	3.0554
p^h, $h = 1/16$	1.8622	1.1119	4.3459	3.4051	2.0469	1.5867	3.7594	3.2026
p^h, $h = 1/32$	1.6394	0.7047	4.5747	3.5151	1.9471	1.4257	4.0405	3.4385
p	0	0	6	6	0	0	6	6

Table 5. Simulation results with four temperature distributions.

Element	1	2	3	4	5	6	7	8
p^h, $h = 1/8$	1.3349	0.2514	5.3724	3.9005	2.0002	1.4610	4.6298	3.8130
p^h, $h = 1/16$	1.0537	0	5.7299	4.0914	1.7936	1.0421	5.0370	4.0996
p^h, $h = 1/32$	0.7388	0	5.8434	4.1310	1.6299	0.7995	5.3400	4.3535
p	0	0	6	6	0	0	6	6

Table 6. Reconstructed source powers.

h	1/8	1/16	1/32
One temperatures	0.1658	0.1666	0.1663
Four temperatures	0.1778	0.1785	0.1784

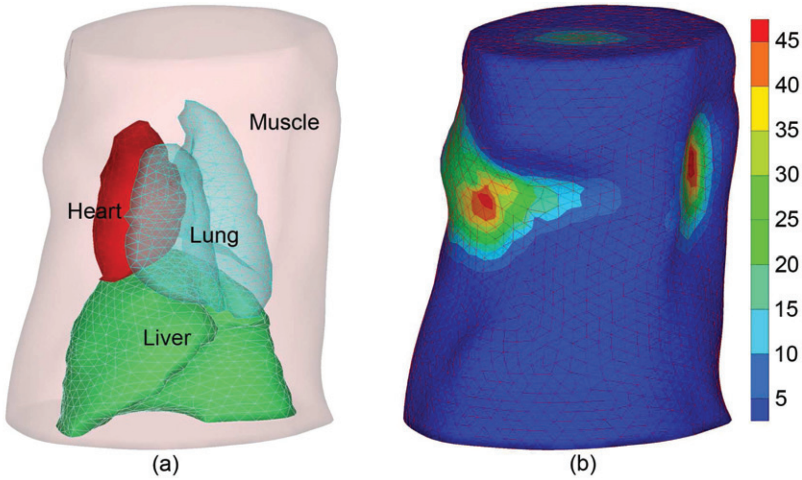

Figure 3. Finite element mouse chest model and associated bioluminescent measurement. (a) A geometrical model of the mouse chest consisting of muscle, a heart, lungs, and a liver, and (b) measured bioluminescent data mapped onto the surface of the finite element mouse chest model.

Table 7. Optical parameters for the mouse organ regions.

Material	Muscle	Lung	Heart	Liver
μ_a (mm^{-1})	0.23	0.35	0.11	0.45
μ_s' (mm^{-1})	1.00	2.30	1.10	2.00

Example 8.2 In this example, we compare the TBT algorithm with the ordinary BLT algorithm using an anatomically realistic digital mouse chest phantom built from an segmented MRI mouse image volume. We obtain a finite-element model, as shown in Figure 3(a), of the digital mouse chest phantom. This phantom consists of lungs, a heart, a liver and muscle. Appropriate absorption μ_a and reduced scattering μ_s' coefficients are assigned to these anatomical structures as shown in Table 7. The finite element model of the digital mouse phantom contains 14,757 nodes and 80,670 tetrahedral elements.

In the simulation, we randomly put a source in a tetrahedral element in a spherical region of $r = 3$ mm, which contains 1111 tetrahedral elements, and centre

Table 8. Simulated TBT results in terms of source localization and power estimation errors.

	Three-temperature	One-temperature
Location error	0.7067 mm	0.8124 mm
Power error	2.52%	5.14%

at (2, 2, 10) mm. In this region, there are 539, 284 and 288 elements belonging to muscle, lung and heart, respectively. We then set the permissible region as a spherical region of $r = 6$ mm, which contains 8792 tetrahedral elements, and centre at (2, 2, 10) mm. To reduce the computational cost, we will only use one spectral. The power of the source will be adjusted to create a moderate surface signal strength (maximum = 50). Figure 3(b) shows a typical surface bioluminescence signal distribution. Then Poisson noise and 20 dB white Gaussian noise will be added to the signal and rounded to the nearest integer. We then apply the TBT algorithm to the one-temperature and three-temperature data sets; the simulation result is shown in Table 8. In this simulation, we do 1000 random runs and the results shown in the table are the average over 1000 random runs. The results show that temperature data can reduce the reconstruction error. Here, the location error is defined to be the distance between the centre of the true source location and the centre of reconstructed source location, the latter being defined as the averaged centre among the centres of all the elements in the permissible region weighted by the constant values of the reconstructed light source function on the elements. The power error is the relative error of the reconstructed source power with respect to the true source power. ■

References

[1] R. Weissleder and U. Mahmood, *Molecular imaging*, Radiology 219 (2001), pp. 316–333.

[2] G. Wang, R. Jaszczak, and J. Basilion, *Towards molecular imaging*, IEEE Trans. Med. Imag. 24 (2005), pp. 829–831.

[3] C.H. Contag and B.D. Ross, *It's not just about anatomy: In vivo bioluminescence imaging as an eyepiece into biology*, J. Magn. Reson. Imag. 16 (2002), pp. 378–387.

[4] R. Weissleder and V. Ntziachristos, *Shedding light onto live molecular targets*, Nat. Med. 9 (2003), pp. 123–128.

[5] V. Ntziachristos, J. Ripoll, L.V. Wang, and R. Weissleder, *Looking and listening to light: the evolution of whole-boday photonic imaging*, Nat. Biotechnol. 23 (2005), pp. 313–320.

[6] V. Ntziachristos, C.H. Tung, C. Bremer, and R. Weissleder, *Fluorescence molecular tomography resolves protease activity in vivo*, Nat. Med. 8 (2002), pp. 757–761.

[7] G. Wang, E.A. Hoffman, G. McLennan, L.V. Wang, M. Suter, and J.F. Meinel, *Development of the first bioluminescent CT scanner*, Radiology 229 (P) (2003), p. 566.

[8] G. Wang, Y. Li, and M. Jiang, *Uniqueness theorems in bioluminescence tomography*, Med. Phys. 31 (2004), pp. 2289–2299.

[9] W.X. Cong, G. Wang, D. Kumar, Y. Liu, M. Jiang, L.H. Wang, E.A. Hoffman, G. McLennan, P.B. McCray, J. Zabner, and A. Cong, *A practical reconstruction method for bioluminescence tomography*, Optics Express 13 (2005), pp. 6756–6771.

[10] W. Han, W.X. Cong, and G. Wang, *Mathematical theory and numerical analysis of bioluminescence tomography*, Inverse Prob. 22 (2006a), pp. 1659–1675.
[11] W. Han, K. Kazmi, W.X. Cong, and G. Wang, *Bioluminescence tomography with optimized optical parameters*, Inverse Prob. 23 (2007), pp. 1215–1228.
[12] W. Han, W.X. Cong, K. Kazmi, and G. Wang, *An integrated solution and analysis of bioluminescence tomography and diffuse optical tomography*, a special issue of Commun. Num. Methods Eng. (2008), DOI: 10.1002/cnm.1163, 18 pages.
[13] X.L. Cheng, R.F. Gong, and W. Han, *A new general mathematical framework for bioluminescence tomography*, Comput. Meth. Appl. Mech. Eng. 197 (2008), pp. 524–535.
[14] X.L. Cheng, R.F. Gong, and W. Han, *Numerical approximation of bioluminescence tomography based on a new formulation*, J. Eng. Math. 63 (2009), pp. 121–133.
[15] W. Han, W.X. Cong, and G. Wang, *Mathematical study and numerical simulation of multispectral bioluminescence tomography*, Int. J. Biom. Imag. 2006 (2006b), Article ID 54390, 10 pages.
[16] W. Han and G. Wang, *Theoretical and numerical analysis on multispectral bioluminescence tomography*, IMA J. Appl. Math. 72 (2007), pp. 67–85.
[17] W. Han and G. Wang, *Bioluminescence tomography: biomedical background, mathematical theory, and numerical approximation*, J. Comput. Math. 26 (2008), pp. 324–335.
[18] H. Zhao, T. Doyle, O. Coquoz, F. Kalish, B. Rice, and C. Contag, *Emission spectra of bioluminescent reporters and interaction with mammalian tissue determine the sensitivity of detection in vivo*, J. Biomed. Opt. 10 (2005), p. 041210.
[19] G. Wang, H. Shen, W.X. Cong, S. Zhao, and G.W. Wei, *Temperature-modulated bioluminescence tomography*, Optics Express 14 (2006), pp. 2289–2299.
[20] K. Atkinson and W. Han, *Theoretical Numerical Analysis: A Functional Analysis Framework*, 2nd ed., Springer-Verlag, New York, 2005.
[21] L.C. Evans, *Partial Differential Equations*, American Mathematical Society, Providence, RI, 1998.
[22] P.G. Ciarlet, *The Finite Element Method for Elliptic Problems*, North Holland, Amsterdam, 1978.